RSC Advances

PAPER

View Article Online
View Journal | View Issue

Cite this: *RSC Adv.*, 2020, **10**, 76

UHPLC-MS metabolome based classification of umbelliferous fruit taxa: a prospect for phyto-equivalency of its different accessions and in response to roasting†

Ahmed Serag, [a] Mostafa H. Baky, [b] Stefanie Döll [c] and Mohamed A. Farag *[de]

Herbs of the Umbelliferae family are popular spices valued worldwide for their many nutritional and health benefits. Herein, five chief umbelliferous fruits *viz.*, cumin, fennel, anise, coriander and caraway were assessed for its secondary metabolites diversity along with compositional changes incurring upon roasting as analyzed *via* ultra-high performance liquid chromatography coupled to photodiode array and electrospray ionization mass detectors UHPLC-qToF/MS. A total of 186 metabolites were annotated, according to metabolomics society guidelines, belonging mainly to flavonoids, fatty acids and phenolic acids. Multivariate models *viz.*, PCA, HCA and OPLS-DA were further employed to assess fruits' heterogeneity in an untargeted manner and determine mechanistic changes in bioactive makeup post roasting *viz.*, glycosidic cleavage, lipid degradation and Maillard reaction. Finally, the fruits' antioxidant activity showed decline upon roasting and in correlation with its total phenolic content. This study presents the first complete map of umbelliferous fruit metabolome, compositional differences and its roasting effect.

Received 26th September 2019
Accepted 14th December 2019

DOI: 10.1039/c9ra07841j

rsc.li/rsc-advances

1. Introduction

Culinary herbs and spices are plants that are used fresh or dry, not only to improve aroma or piquancy of food and drinks, but also for their nutritive and health promoting effects. The Umbelliferae family (*Apiaceae*) is one of the largest taxa among higher plants with more than 300 genera and 3000 species that are indigenous to the Mediterranean basin and distributed in central Asia and Europe.[1] Owing to a myriad of sensory metabolites and phytochemical constituents, members of this family are well recognized for their use in traditional medicine, culinary use, beverages and in cosmetics.[2] Among umbelliferous plants, *Cuminum cyminum* L. (cumin), *Foeniculum vulgare* Miller (fennel), *Pimpinella anisum* L. (anise), *Coriandrum sativum* L. (coriander) and *Carum carvi* L. (caraway) are the most common aromatic spices used in different cuisines worldwide. Apart from serving as spices, they have been the target of many research work for their health benefits as anti-tumor, antimicrobial, anti-inflammatory, digestive, antispasmodic, estrogenic, hypoglycemic, radical scavenging and hypolipidemic activities.[3] Chemical classes present in Umbelliferae fruits and to mediate for these effects include a plethora of metabolites *viz.*, essential oil, flavonoids, coumarins, phenolic acids, fatty acids, terpenes, stilbenes and sterols.[2]

Roasting is one of the most common processes used to improve food quality *viz.*, aroma, flavor and color concurrent with several reactions to occur such as Maillard reaction or lipid degradation which could lead to the generation of a different bioactive profile from the unroasted plant. For example, studies revealed that roasting could affect the total phenolic composition and antioxidant activity of herbs and spices mostly accompanied by a substantial loss of their antioxidant activity.[4] Hence, a holistic approach is warranted to unveil the changes occurring during the roasting process rather than analysis of a single component or specific class of compounds in order to ensure food quality and safety for the consumers and industry as well.[5]

Metabolomics is a unique tool in modern systems biology that has been recently employed for fingerprinting and/or profiling the overall chemical makeup of plant-derived food.[6] Detecting food components on a molecular level offers valuable insights into the complex relationships of bioactive

[a]*Pharmaceutical Analytical Chemistry Department, Faculty of Pharmacy, Al-Azhar University, Cairo, 11751, Egypt*

[b]*Pharmacognosy Department, Faculty of Pharmacy, Egyptian Russian University, Cairo, 11829, Egypt*

[c]*Department of Stress and Developmental Biology, Leibniz Institute of Plant Biochemistry, Weinberg 3, D-06120 Halle (Saale), Germany*

[d]*Pharmacognosy Department, Faculty of Pharmacy, Cairo University, Cairo, 11562, Egypt. E-mail: Mohamed.farag@pharma.cu.edu.eg*

[e]*Chemistry Department, School of Sciences & Engineering, The American University in Cairo, New Cairo, Egypt*

† Electronic supplementary information (ESI) available. See DOI: 10.1039/c9ra07841j

phytochemicals and their nutritive and therapeutic effects.[7] For non-volatile polar secondary metabolites profiling, metabolomics mostly employ hyphenated techniques such as state of the art ultra-high performance liquid chromatography (UHPLC) with high resolution quadrupole-time of flight (Q-TOF) mass analyzer. Compared to conventional low resolution LC-MS, UHPLC-QToF/MS offers several advantages in metabolomics experiments including higher efficiency, excellent resolution with relatively short analysis times in addition to higher mass accuracy, the latter advantage warrants resolving of the isomeric and isobaric species, and last but not least, another data dimension with the highly informative fragmentation pattern from MS/MS runs represents key steps in metabolite identification.[8] Hence, high throughput UHPLC/MS based metabolomics has been used extensively to investigate phytochemical variations across different plant genera as well as closely allied species and taxa.[9] Furthermore, it has been also utilized for assessing changes incurring as a results of food processing as typical in many of its products.[10] A metabolomics study revealed that roasting led to increased levels of proline derivatives *viz.*, betonicine, *N*-methylproline and stachydrine in peanuts suggestive for changes in their amino acid pattern.[11]

We have previously reported a metabolomics study[12] assessing umbelliferous fruits' aroma profiles using headspace solid phase microextraction gas chromatography mass spectrometry (SPME-GC/MS) targeting its aroma compounds. This approach revealed several newly-occurring volatile classes such as pyrazines, furans and pyrans being detected upon roasting. Extending our work on umbelliferous fruits, we present herein the first map of umbelliferous fruits' secondary metabolites profile for (a) its chemical taxonomy as well as (b) to scrutinize roasting impact on its phytochemicals that mediate for its health benefits *via* UHPLC-QToF/MS and (c) relate metabolite profile results to antioxidant effects in these fruits. Owing to the complexity of the data generated in such high throughput analysis comprising several specimens, data mining algorithms seem imperative. Hence, multivariate data analysis such as unsupervised methods *viz.*, principal component analysis (PCA) and hierarchical clustering analysis (HCA) in addition to supervised methods *viz.*, orthogonal projection to least squares-discriminant analysis (OPLS-DA) were employed to unravel the heterogeneity in addition for markers discovery post roasting process. Furthermore, antioxidant assays were employed to evaluate the impact of roasting on fruits in correlation to total phenolics and flavonoids content.

2. Materials and methods

2.1. Plant material

Five umbelliferous fruits *viz. Cuminum cyminum*, *Foeniculum vulgare*, *Pimpinella anisum*, *Coriandrum sativum* and *Carum carvi* were procured from plants grown at the Faculty of Pharmacy Herbarium, Cairo University, Giza, Egypt. The fruits were finely powdered and stored at −20 °C till further analysis. Three biological replicates were analyzed for each sample. Voucher specimens were deposited at Pharmacognosy Department, Faculty of Pharmacy, Cairo University. The effect of the roasting procedures was assessed by heating 20 g fruits (*Cuminum cyminum*, *Foeniculum vulgare* and *Pimpinella anisum*) in an oven set at 180 °C for 12 min with occasional stirring. All experiments were performed in 3 biological triplicates.

2.2. Chemicals and reagents

Acetonitrile and formic acid (LC-MS grade) were obtained from J. T. Baker (The Netherlands); Milli-Q water was used for UHPLC analysis. Chromoband C18 (500 mg, 3 mL) cartridge was purchased from Macherey-Nagel (Düren, Germany). All other chemicals and standards were purchased from Sigma-Aldrich (St Louis, MO, USA).

2.3. Preparation of fruit extracts for UHPLC-MS analysis

The extraction of the umbelliferous fruit metabolome was performed as previously described in our previous work.[13] Briefly, the freeze dried fruits were ground with a pestle in a mortar, then 2 g of each fruit powder was homogenized with 5 mL 100% MeOH containing 10 μg mL^{-1} umbelliferone (an internal standard used for relative quantification of UHPLC-MS features) using a Turrax mixer (11 000 rpm) for five 20 second periods with recession time of 1 min. Extracts were then vortexed vigorously and centrifuged at 3000 g for 30 min to remove plant debris. For solid phase extraction, 500 μL were aliquoted and loaded on a (500 mg) C18 cartridge which was preconditioned with methanol and water. Samples were then eluted with of 3 mL 70% MeOH and 3 mL 100% MeOH, the eluents were evaporated to dryness under a gentle nitrogen stream. The obtained dry residue was re-suspended in 500 μL methanol for further UHPLC-MS analysis.

2.4. High-resolution UHPLC-MS analysis

The analytical conditions for high resolution UHPLC-MS were employed as previously described in our previous work.[14] The UHPLC analysis was performed on an Acquity UHPLC System (Waters) equipped with a HSS T3 column (100 × 1.0 mm, particle size 1.8 μm; Waters). The analysis was carried out by applying the following binary gradient at a flow rate of 150 μL min^{-1}: 0–1 min, isocratic 95% A (water/formic acid, 99.9/0.1 [v/v]), 5% B (acetonitrile/formic acid, 99.9/0.1 [v/v]); 1–16 min, linear from 5 to 95% B; 16–18 min, isocratic 95% B; and 18–20 min, isocratic 5% B. The injection volume was 3.1 μL (full loop injection). Eluted compounds were detected from *m*/*z* 90 to 1000 using a MicroTOF-Q hybrid quadrupole time-of flight mass spectrometer (Bruker Daltonics) equipped with an Apollo-II electrospray ion source in negative and positive (deviating values in brackets) ion modes using the following instrument settings: nebulizer gas, nitrogen, 1.4 (1.6 bar); dry gas, nitrogen, 6.l min^{-1}, 190 °C; capillary, −5000 V (+4000 V); end plate offset, 500 V; funnel 1 RF, 200 Vpp; funnel 2 RF, 200 Vpp; in-source CID energy, 0 V; hexapole RF, 100 Vpp; quadrupole ion energy, 5 eV (3 eV); collision gas, argon; collision energy, 7 eV (3 eV); collision RF, stepping 150/350 Vpp (200/300 Vpp), (timing 50/50); transfer time, 58.3 μs; prepulse storage, 5 μs; pulser frequency, 10 kHz; and spectra rate, 3 Hz. Internal mass calibration of each analysis was performed by infusion of 20 μL 10 mM lithium formate

in isopropanol : water, 1 : 1 (v/v), at a gradient time of 18 min using a diverter valve.

For Auto-MS/MS analysis, precursor ions were selected in Q1 with an isolation width of ±3–10 Da and fragmented at collision energies of 15–70 eV using argon as a collision gas. Product ions detection was performed using the same settings as above, but with funnel 2 RF 300 Vpp in negative mode. Metabolites were characterized by their UV-vis spectra (210–650 nm), retention times relative to external standards, accurate MS and the domino MS/MS spectra in comparison to our in-house database, phytochemical dictionary of natural products database and reference literature. Confidence levels of annotation were reported according to the guidelines of the metabolomics society compound identification work group at their 2017 annual meeting (Brisbane, Australia).[15]

2.5. MS data processing for multivariate data analysis

Features extraction of the examined umbelliferous fruits MS files was performed using XCMS package under R 2.9.2 environment. The script employed for peak detection, alignment and grouping of the extracted ion chromatograms is presented in (ESI Code S1†) and follows the following the exact procedure described in.[16] Normalization and Pareto scaling of the features prior to modelling were performed using the Microsoft Excel software where multivariate models PCA, HCA and OPLS-DA were performed with the program SIMCA-P Version 13.0 (Umetrics, Umea, Sweden).

2.6. Total phenolics content

The total phenolic content (TPC) was estimated using the Folin–Ciocalteu colorimetric method according to ref. 17 with minor modifications. Briefly, mixtures of 0.1 mL of plant extracts prepared at a concentration of 1 mg mL^{-1}, 0.1 mL of 0.5 N Folin–Ciocâlteu and 1 mL of sodium carbonate (Na_2CO_3, 75 g L^{-1}) was allowed to stand for 90 min in the dark at room temperature. Absorbance of the resulting blue color was measured at 760 nm using JASCO v-630 (USA) spectrophotometer. Gallic acid was used as a reference standard and the results were expressed as gram of gallic acid equivalents (GAE) per g dry extract of plant.

2.7. Total flavonoids content

The total flavonoids content (TFC) for anise, fennel and cumin pre and post roasting were determined. Briefly, a 1 mL aliquot of 2% $AlCl_3$ aqueous solution was mixed with 1 mL of each sample prepared at a concentration of 1 mg mL^{-1}. After an incubation time of 30 min, samples absorbance was measured at 420 nm.[18] Quercetin was used as a reference standard and the TFC is calculated as quercetin equivalents (QE) in mg g^{-1} dry weight of plant material extract.

2.8. DPPH˙ radical scavenging activity

Radical scavenging activity of the examined fruits against DPPH˙ (2,2-diphenyl-2-picrylhydrazyl hydrate) free radical was determined spectrophotometrically. Fixed volume (100 μL) of different concentrations of the studied fruits (50–1000 μg mL^{-1}) was added to 3.9 mL of 0.2 mM DPPH˙ and allowed to stand in the dark for 60 min. Reduction in the DPPH˙ radical was determined by measuring decrease in absorbance at 515 nm. Ascorbic acid was used as a positive control and the results were expressed as % inhibition for DPPH˙. IC_{50} for each sample was calculated and compared to that of ascorbic acid.[17]

3. Results & discussion

3.1. Secondary metabolites profiling in fruits *via* UHPLC-PDA-ESI-QToF/MS

In the present study, untargeted high resolution UHPLC-PDA-ESI-QToF/MS metabolomics approach was employed to assess secondary metabolites heterogeneity among major umbelliferous fruits *viz.*, cumin, fennel, anise, caraway and coriander. A gradient mobile phase of acetonitrile with aqueous formic acid allowed for the comprehensive elution of all metabolite classes *viz.*, phenolic acids, coumarins, flavonoids, sphingolipids and fatty acids within *ca.* 18 min. Fruit extracts were analyzed in both negative and positive electrospray ionization modes to provide a comprehensive view of their metabolite composition. The negative-ion MS spectra accounted for more sensitive identification of polar phenolic acids, flavonoids and fatty acids with more observable peaks belonging to these classes due to the presence of phenyl or carboxyl groups which preferentially ionize much better in the negative ionization mode. On the other hand, the positive-ion MS spectra performed better for acylated amino acids, fatty acid amides and some sphingolipids as these compounds bear a nitrogen atom which show better ionization and detection in the positive mode. The acquired UHPLC-MS traces for umbelliferous fruits in both ionization modes in addition to the traces of the roasted species are depicted in Fig. 1 in addition to (ESI Fig. S1–S3†) with two main regions: the first half (30–400 s) for peaks mainly belonging to acylated amino acids, phenolic acids, coumarins, stilbenes, terpenes and flavonoids. The later elution region (420–1000 s) showed peaks mainly due to non-polar sphingolipids and fatty acids along with their amides. The retention time, experimental *m*/*z*, molecular formula, mass error, UV characteristics, main MS^2 fragments and identities for individual peaks are all compiled in (ESI Table S1†). A total of 186 metabolites were annotated, of which 145 were tentatively identified using strict confidence levels according to the metabolomics society guidelines; predominating classes were flavonoids, fatty acids and phenolic acids as depicted in Fig. 2. To the best of our knowledge, this is the first comprehensive metabolite profiling of umbelliferous fruits used as spices that help provide chemical based evidence for their nutritive and or health benefits. The basic structures of metabolites detected in the studied specimens and discussed throughout the manuscript are illustrated in Fig. S4.†

3.1.1. Phenolic acids. Thirty-eight phenolic acids including several glycosylated and ester forms of hydroxy benzoic and hydroxy cinnamic acids represent one of the major classes found in all examined fruits. In detail, 4-acylated hydroxy benzoic acid hexosides were detected from a loss of 162 amu

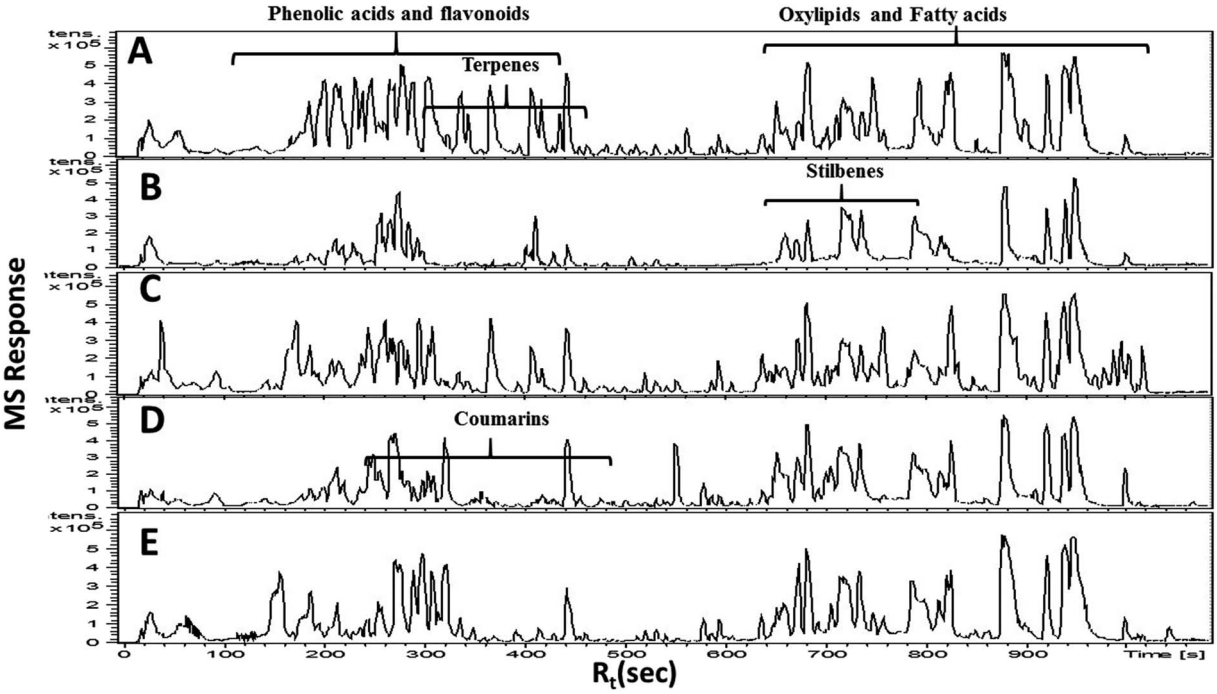

Fig. 1 Representative UHPLC-MS traces analyzed in the negative ion mode of unroasted methanol extracts of cumin (A), fennel (B), anise (C), coriander (D) and caraway (E), characterized by 2 main regions: (150–400 s) with peaks mainly due to phenolic acids and flavonoids and a region (550–1000 s) assigned for oxylipids and fatty acids.

(hexose) identified as di-hydroxybenzoic acid-*O*-hexoside (7), vanillic acid-*O*-hexoside (8), syringic acid-*O*-hexoside (12) and hydroxybenzoic acid-*O*-hexoside (19). Similarly, peaks 14, 16, 29 and 37 were assigned as the hexoside conjugates of caffeic, coumaric, ferulic and sinapic acids with characteristic fragments at *m*/*z* 179, 163, 193 and 223, respectively, corresponding to its aglycon part. Free hydroxycinnamic acids may occur in many fruits and vegetables during their processing or when the plant encounter physiological disturbances or contamination by microorganisms.[19]

Rosmarinic acid (84), a caffeic acid ester with potential anti-inflammatory and acetylcholinesterase inhibitor activities, was found exclusively in fennel in agreement with previous report.[20] Rosmarinic acid displayed $[M - H]^-$ at *m*/*z* (359.0767, $C_{18}H_{15}O_8^-$) with MS/MS fragment ions (ESI Fig. S5a†) at *m*/*z* 197 and 161. Furthermore, cumic acid (123) was detected exclusively in cumin samples at *m*/*z* (163.0765, $C_{10}H_{11}O_2^-$) with MS^2 spectrum characterized by loss of methyl, ethyl and isopropyl moieties to exhibit fragments at *m*/*z* 148, 134 and 121, respectively.

In addition, three hydroxycinnamic acid esterified with quinic acid were detected in peaks 11, 20 and 26 with the same $[M - H]^-$ at *m*/*z* (353.0878, $C_{16}H_{17}O_9^-$) and UV lambda max of 323 nm, assigned as *O*-caffeoyl quinic acid isomers (ESI Fig. S5b†), found in all the examined umbelliferous fruits with potential radical scavenging, anticancer, antibacterial and antihypertensive activities.[21]

Likewise, two peaks 36 and 46 with *m*/*z* (337.0934, $C_{16}H_{17}O_8^-$) and (367.1027, $C_{17}H_{19}O_9^-$), characterized by loss of the coumaroyl (M − H-162) and feruolyl (M − H-193) moieties, were identified as *O*-coumaroyl quinic acid and *O*-feruloyl quinic acid, respectively (ESI Fig. S5c and d†). In addition, peak 69 displayed $[M - H]^-$ at *m*/*z* (515.1188, $C_{25}H_{23}O_{12}^-$) was assigned as di-*O*-caffeoylquinic acid based on its characteristic fragmentation pattern (ESI Fig. S5e†), first time to be reported in anise and fennel. A related analogue for di-*O*-caffeoylquinic acid was identified in peaks 93 and 99 with the same $[M - H]^-$ at *m*/*z* (529.1351, $C_{26}H_{25}O_{12}^-$) and assigned as *O*-caffeoyl-*O*-feruloylquinic acid isomers (ESI Fig. S5f†) and exhibiting fragment ions at *m*/*z* 179, 161, 135 indicative for caffeic acid moiety *versus* fragments at *m*/*z* 193 and 191 due to ferulic and quinic acid moieties, respectively. Finally, two positional isomer peaks 89 and 97 exhibited $[M - H]^-$ at *m*/*z* (499.1232, $C_{25}H_{23}O_{11}^-$) and yielding fragment ions (ESI Fig. S5g†) at *m*/*z* 191, 163 and 119 corresponding to quinic acid, dihydroxy-cinnamoyl and hydroxy-cinnamoyl moieties, respectively assigned as positional isomers for *O*-(dihydroxy-cinnamoyl)-*O*-(hydroxy-cinnamoyl) quinic acid isomers, first time to be reported in anise.

3.1.2. Flavonoids. Flavonoids are well-known to be an important part of the diet due to their many health-promoting benefits including antioxidant activity, reduced risk of cancer in addition to mitigating against neurodegenerative diseases.

In this study, a total of 42 flavonoid peaks belonging to two main subclasses *i.e.* flavones and flavonols were tentatively characterized based on their characteristic UV spectra. The identified flavonoids were free, glycosylated and/or acylated derivatives with characteristic MS/MS fragmentation pattern depending on the sugar type *i.e.* hexose *versus* deoxyhexose,

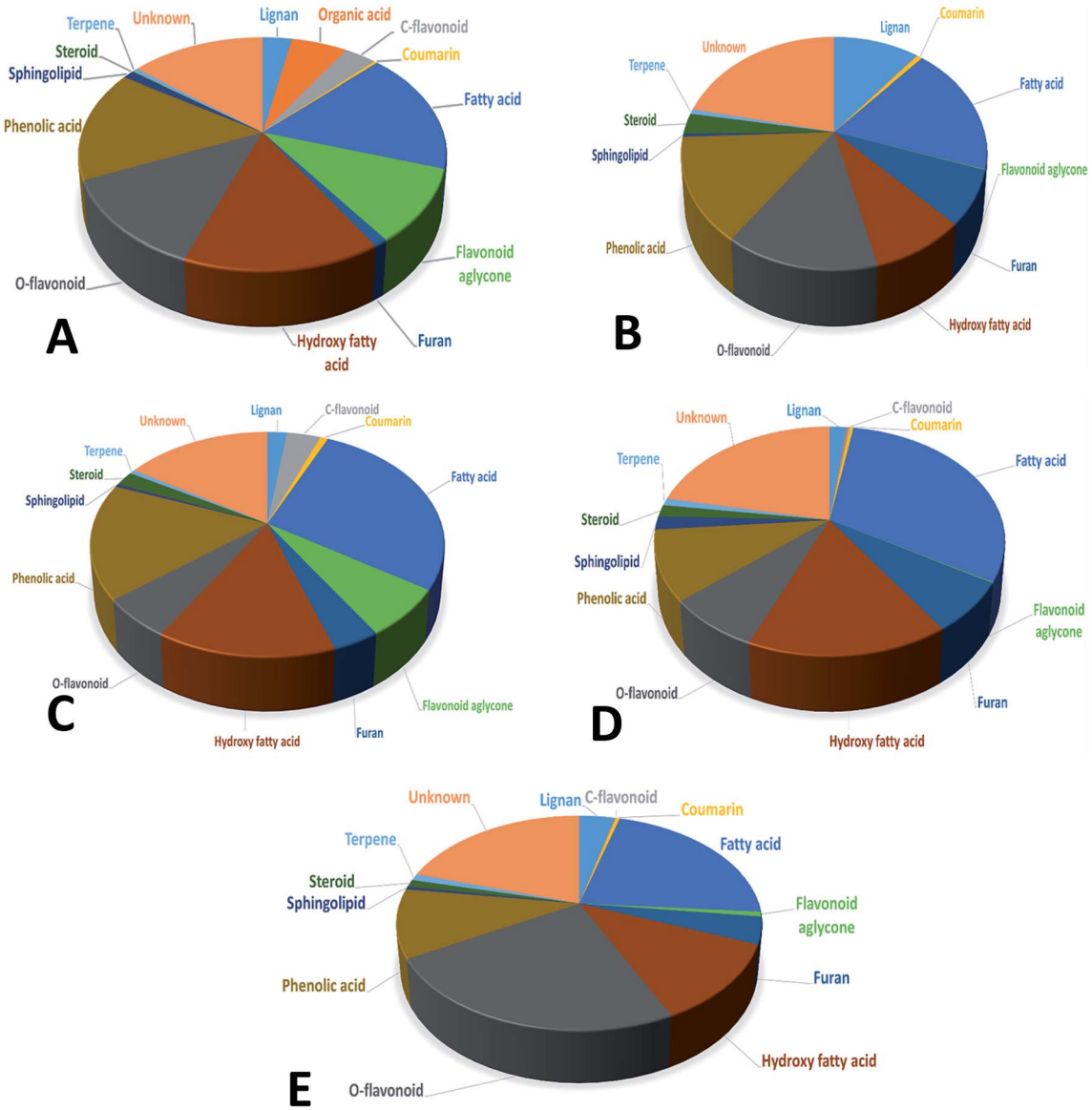

Fig. 2 Mean relative percentile levels of the main chemical classes in unroasted cumin (A), fennel (B), anise (C), coriander (D) and caraway (E), according to identified features from the LC-MS dataset.

linking atom *i.e. O versus C*-glycoside and site of attachment *i.e.*, 6 *versus* 8 position in the aglycone part. In that context, 5 free flavonoid aglycones were detected in peaks (102, 104, 113, 116 and 119) corresponding to quercetin *m*/*z* (301.035, $C_{15}H_9O_7^-$), luteolin at *m*/*z* (285.0412, $C_{15}H_9O_6^-$), apigenin at *m*/*z* (269.0467, $C_{15}H_9O_5^-$), kaempferol at *m*/*z* (285.0384, $C_{15}H_9O_6^-$) and chrysoeriol at *m*/*z* (299.0559, $C_{16}H_{11}O_6^-$), respectively. Identification of *O*-type flavonoid glycosides could be revealed based on the homolytic cleavage of its *O*-glycosidic bond leading to neutral loss of the sugar residues that are either hexose, deoxyhexose, pentose and hexouronic acid with a respective loss of 162, 146, 132 and 176 amu.[22] In contrast, *C*-type flavonoid glycosides exhibit non-homogenous fragments due to 0,2 and 0,3 cross-ring cleavages of the sugar moieties leading to loss of 120 & 90 amu in *C*-hexosides *versus* 90 & 60 amu in *C*-pentosides and 104 & 74 amu in *C*-deoxyhexosides.

Within *C*-glycosides, 4 apigenin based glycosides were detected including apigenin di-*C*-hexoside (38), apigenin di-*C*-pentoside (58), apigenin *C*-hexoside (62) and apigenin-*C*-hexosyl-*C*-rhamnoside (86) mostly found in coriander and cumin samples. Fragmentation for these *C*-flavonoids were consistent with the non-homogenous cleavage previously mentioned, for example peak 38 with $[M - H]^-$ at *m*/*z* (593.1514, $C_{27}H_{29}O_{15}^-$) and further fragmenting to yield (ESI Fig. S6a†) *m*/*z* 473 (M − H-120), 413 (M − H-180), 383 (A + 113) and 353 (A + 83) typifying apigenin di-*C*-hexoside. Additionally, two luteolin-*C*-glycosides in peaks 50 and 51 were also characterized in anise and coriander assigned as luteolin-6-*C*-hexosyl-8-*C*-pentoside and luteolin-*C*-hexoside (ESI Fig. S6b†). It should be noted that *C*-glycosides were represented by few peaks found mainly in coriander, cumin and anise samples, and all of flavone subclass

suggesting for *C*-glycosidic activity with high substrate specificity towards only flavones in these umbelliferous fruits.

In contrast, O-type flavonoids amounted as the dominant flavonoids present in all examined umbelliferous fruits. 7 Glycosylated flavones comprising luteolin (peaks 53, 70, 85 and 92) and apigenin (peaks 59, 72 and 75)-*O*-glycosides were characterized as revealed from *m*/*z* (285, $C_{15}H_9O_6^-$) and (269, $C_{15}H_9O_5^-$) corresponding to luteolin and apigenin aglycones, respectively. Moreover, two methoxylated flavone conjugates (peaks 63 and 82) were detected exclusively and for the first time in cumin annotated as chrysoeriol-*O*-hexosyl hexauronide and chryseriol-*O*-hexoside with $[M - H]^-$ at *m*/*z* (637.1439, $C_{28}H_{29}O_{17}^-$) and (461.1107, $C_{22}H_{21}O_{11}^-$), respectively. Confirmation of chrysoeriol as agylcone moiety was gained from MS^2 fragment ions (ESI Fig. S7a and b†) at *m*/*z* 299 and 298 ascribed to the aglycone moiety and its radical ion and further showing a loss of 15 amu of its methoxy group. Methoxylated flavonoids are known to be superior to their hydroxylated counterparts regarding their biological effects as methylation protects these compounds from hepatic metabolism and increases their intestinal absorption and cellular binding, thus promoting their pharmacological activity.[23]

Similarly, MS spectra interpretation allowed for the detection of flavonol glycosides *viz.*, quercetin (*m*/*z* 301.0352, $C_{15}H_9O_7^-$) in peaks (61, 64 and 65) and kaempferol (*m*/*z* 285.0329, $C_{15}H_9O_6^-$) in peaks (68 and 94) mostly in fennel and coriander samples. Quercetin is the most potent scavenger of the reactive oxygen species within the flavonoid family *via* its catechol group in the B ring and the OH group at position 3 of the AC ring. The optimal configuration for these pharmacophore groups to scavenge free radicals empowered such potent activity. Moreover, peak 73 $[M - H]^-$ at *m*/*z* (477.1018, $C_{22}H_{21}O_{12}^-$) was annotated as isorhamnetin-*O*-hexoside, a methylated derivative of quercetin reported to occur in fennel, with MS^2 spectrum (ESI Fig. S8a†) at *m*/*z* 314 (M − H-162) and 299 corresponding to loss of the methyl group from the isorhamnetin aglycon. Additionally, several acyl flavonoids including acetyl and malonyl derivatives were identified in peaks (74, 79, 80 and 106) and peaks (67, 77 and 95), as evident from the loss of 42 and 86 amu, respectively, detected mainly in caraway and cumin samples. Interestingly, novel acylated glycosides containing hydroxy cinnamic acids in quercetin peak (87) and luteolin peak (105) are first time to be reported in caraway. In detail, compound 87 displayed $[M - H]^-$ at *m*/*z* (625.1185, $C_{30}H_{25}O_{15}^-$) annotated as quercetin-*O*-caffeoyl-hexoside with MS^2 spectrum (ESI Fig. S8b†) of daughter ions at *m*/*z* 463 (M − H-162) indicative for loss of a hexose moiety and *m*/*z* 161 indicative for caffeoyl-H_2O moiety. Luteolin-*O*-feruloyl-hexoside (peak 105; 623.1371, $C_{31}H_{27}O_{14}^-$) exhibited MS^2 fragment at *m*/*z* 284 corresponding to luteolin radical anion. Finally, cuminoid E, a chalcone compound with potential hypoglycemic activity previously reported in cumin,[24] was also characterized displaying $[M - H]^-$ at *m*/*z* (473.1469, $C_{24}H_{25}O_{10}^-$) and showing loss of hexose, methoxy and carboxylate group (ESI Fig. S9†) at *m*/*z* 311 (M-H-162), 279 ($-OCH_3$) and 235 ($-CO_2$), respectively. The versatility and exquisite substrate and site specificity of flavonoid modifying enzymes, as well as the divergent roles of different flavonoid derivatives in plant food, is a topic of recent investigation.

3.1.3. Fatty acids and sphingolipids. Next to flavonoids and phenolic acids, fatty acids amounted as the third abundant class in umbelliferous represented by a total of 37 peaks and predominated by poly unsaturated and hydroxylated forms. In details, peaks 161 (*m*/*z* 277.2184, $C_{18}H_{29}O_2^-$), 169 (*m*/*z* 279.2322, $C_{18}H_{31}O_2^-$), 174 (*m*/*z* 255.2331, $C_{16}H_{31}O_2^-$), 175 (*m*/*z* 281.2496, $C_{18}H_{33}O_2^-$), 181 (*m*/*z* 283.2645, $C_{18}H_{35}O_2^-$) and 186 (*m*/*z* 311.295, $C_{20}H_{39}O_2^-$) were found common in all examined fruits and annotated as linolenic acid, linoleic acid, palmitic acid, oleic acid, stearic acid and arachidic acid, respectively. Linolenic and linoleic acid are essential fatty acids which possess anti-inflammatory properties through providing the building blocks for prostaglandins.[25] Interestingly, 4 fatty acids were found exclusively in fennel *viz.*, myristic acid (peak 160; 227.2008, $C_{14}H_{27}O_2^-$), pentadecanoic acid (peak 168; 241.2158, $C_{15}H_{29}O_2^-$), docosanedioic acid (peak 170; 369.3002, $C_{22}H_{41}O_4^-$) and heptadecanoic acid (peak 177; 269.2481, $C_{17}H_{33}O_2^-$) suggesting for abundance of saturated fatty acids in fennel compared to other fruit species. Such results warrant for evaluating its effect on human lipid profile if consumed over long duration.

Furthermore, several hydroxylated fatty acids were detected as major peaks and showing extra loss of water molecules. They are known to possess anti-neuroinflammatory effects in addition to their antimicrobial and cytotoxic activity.[26] In details, trihydroxy-fatty acids were found almost in all the examined fruits *viz.*, trihydroxy-octadecadienoic acid (117), trihydroxy-octadecanoic acid (121) and trihydroxy-octadecanoic acid (122) with exact masses of *m*/*z* (327.2181, $C_{18}H_{31}O_5^-$), (329.2321, $C_{18}H_{33}O_5^-$) and (331.248, $C_{18}H_{35}O_5^-$), respectively. Trihydroxy-octadecanoic acid showed main MS/MS fragments (ESI Fig. S10†) at *m*/*z* 311 and 293 due to subsequent loss of two water molecules and a main fragment at *m*/*z* 211 due to the C15\C16 bond cleavage. Similarly, compounds 127 (*m*/*z* 309.2055, $C_{18}H_{29}O_4^-$), 134 (*m*/*z* 311.2221, $C_{18}H_{31}O_4^-$), 141 (*m*/*z* 313.2383, $C_{18}H_{33}O_4^-$) and 149 (*m*/*z* 315.254, $C_{18}H_{35}O_4^-$) were tentatively characterized as dihydroxy derivatives of octadecatrienoic acid, octadecadienoic acid, octadecenoic acid and octadecanoic acid, respectively, with 2 amu mass differences indicative for the extra double bonds. Besides, MS also revealed several monohydroxy-fatty acids including hydroxy-octadecadienoic acid (peak 151; 295.2277, $C_{18}H_{31}O_3^-$), hydroxy-linolenic acid (peak 155; 293.2112, $C_{18}H_{29}O_3^-$), hydroxyoctadecenoic acid (peak 158; 297.2459, $C_{18}H_{33}O_3^-$) and hydroxy-palmitic acid (peak 159; 271.2273, $C_{16}H_{31}O_3^-$).

Several peaks were detected mostly in fennel and anise samples with an even mass weight in the negative ionization mode of *m*/*z* (564.3342, $C_{27}H_{51}O_9NP^-$), (540.3273, $C_{25}H_{51}O_9NP^-$) and (566.3459, $C_{27}H_{53}O_9NP^-$) tentatively assigned as sphingolipids with characteristic loss of 285 amu indicative for sphingosine moiety. Additionally, free long chain bases of amino alcohols, another class of sphingolipids, were also characterized mostly in fennel using the positive ionization mode including amino-hexadecanediol (peak 129; 274.274, $C_{16}H_{36}NO_2^+$), amino-methyl-heptadecanetriol (peak 131;

318.2992, $C_{18}H_{40}NO_3^+$) and amino-octadecanediol (peak 140; 302.3049, $C_{18}H_{40}NO_3^+$).

3.1.4. Nitrogenous compounds. Three acylated amino acid derivatives were identified in all umbelliferous samples including fructosyl-*O*-valine (3), isoleucyl-*O*-hexose (4) and fructosyl-*O*-phenylalanine (6) with MS/MS spectra showed subsequent loss of water molecules (-2×18) in addition to the sugar loss of 162 amu. Furthermore, another nitrogenous compound was identified exclusively in fennel assigned as pantothenic acid-*O*-hexoside, a vitamin B5 derivative with, with $[M - H]^-$ at *m*/*z* (380.1547, $C_{15}H_{26}NO_{10}^-$) and yielding product ions (ESI Fig. S11†) at *m*/*z* 200 corresponding to pantothenic acid in addition to *m*/*z* 146 due to further losses of CO and CO_2 moieties from pantothenic acid. Pantothenic acid is essential for the metabolic processes as it helps breaking down complex carbohydrates and fats to energize the body and maintain stamina.[27]

Several non-polar fatty acid amides were also identified exclusively in cumin and coriander samples *via* positive ionization mode as indicated from their even mass weights suggesting the presence of nitrogen atom in their structure including oleamide (peak 166; *m*/*z* 282.2767, $C_{18}H_{36}NO^+$), stearamide (peak 176; *m*/*z* 284.293, $C_{18}H_{38}NO^+$), eicosenamide (peak178; *m*/*z* 310.3104, $C_{20}H_{40}NO^+$) and henicosanamide (peak 180; *m*/*z* 326.3424, $C_{21}H_{44}NO^+$).

3.1.5. Coumarins. Esculin, a coumarin glycoside with broad spectrum of pharmacological activity including anti-inflammatory, anticoagulant and anti-tumour effects, was identified in peak 18 on the basis of its $[M - H]^-$ at *m*/*z* (339.0718, $C_{15}H_{15}O_9^-$) and aglycone peak for esculetin at *m*/*z* 177 (ESI Fig. S12†). Furthermore, two furanocoumarins isomers were detected in all studied species (peaks 107 and 108) with $[M - H]^-$ at *m*/*z* (245.0444, $C_{13}H_9O_5^-$) and displaying fragment ions corresponding to successive loss of CH_3 and CO moieties at *m*/*z* 191, and 119, respectively assigned as positional isomers for pimpinellin. The latter compounds were reported to be cytotoxic against the human stomach cancer (MGC-803), prostate cancer (PC3), and malignant melanoma (A375) cell lines *via* the induction of tumor cell apoptosis.[28]

3.1.6. Terpenoids. Whilst extensive reports have been made on umbelliferous volatile terpenes *via* GC/MS, we focus here on the non-volatile forms as analysed using UHPLC/MS. Among different umbelliferous fruits, cumin is well-known to accumulate different terpenoidal compounds accounting for its potential hypoglycemic effect *viz.*, cuminoside A–D.[24] In that context, cuminoid C and cuminoid D were characterized in this study (peaks 42 and 47) with $[M - H]^-$ at *m*/*z* (341.1259, $C_{16}H_{21}O_8^-$) and (343.1406, $C_{16}H_{23}O_8^-$), respectively, and exhibiting MS^2 fragments at *m*/*z* 161 and 163 corresponding to a loss of hexose moiety (ESI Fig. S13a and b†). Additionally, two related monoterpenoidal glycosides were also detected in cumin fruit with respective exact masses of *m*/*z* (347.1713, $C_{16}H_{27}O_8^-$) and (331.178, $C_{16}H_{27}O_7^-$) identified as *p*-menth-ene-triol-*O*-hexoside and *p*-menth-ene-diol-*O*-hexoside, respectively, with a mass difference of 16 amu indicative for extra hydroxyl group.

3.1.7. Stilbenes. Stilbenes have been previously reported in fennel in agreement with our findings in this study. A resveratrol trimer "Miyabenol C" (115) and its glycosidic conjugate (98), were annotated with *m*/*z* (679.1994, $C_{42}H_{31}O_9^-$) and (841.2511, $C_{48}H_{41}O_{14}^-$), respectively. MS/MS spectra of miyabenol C displayed high intensity product ion signals (ESI Fig. S14†) at *m*/*z* 572 (loss of C_7H_6O), 451 (loss of C_7H_6O, C_6H_6O and CO) and *m*/*z* 345.08 (loss of C_7H_6O from 451) and in agreement with fragmentation pattern previously reported.[29]

Additionally, the MS/MS spectrum of peak 56 exhibited fragment ions at *m*/*z* 227, which was observed as the base peak corresponding to the trihydroxystilbene aglycon fragment and affirming the loss of a hexose unit from the deprotonated precursor ion at *m*/*z* (389.1218, $C_{20}H_{21}O_8^-$) and annotated as trihydroxystilbene-*O*-glucoside. Stilbenes are well-known for their potential antioxidant and protein kinase C inhibitor activities which are useful in treating hyperproliferative or inflammatory skin diseases.[30]

3.2. Multivariate data analysis of UHPLC-MS metabolome of umbelliferous fruits

To better visualize metabolite heterogeneity among the examined umbelliferous fruits, two unsupervised pattern recognition tools, namely, principal component analysis (PCA) and hierarchical cluster analysis (HCA) were employed. These tools provide better comprehension of the metabolome structure enabling the detection of heterogeneity among specimens in an unbiased manner.[31] Moreover, a supervised classifier, orthogonal projection to least squares-discriminant analysis (OPLS-DA) was further employed to assess the impact of roasting on three of the examined fruits metabolome. OPLS-DA supersedes PCA in the discriminating ability and markers discovery.

3.2.1. Unsupervised PCA and HCA analysis of umbelliferous fruits. HCA is a statistical method that imposes the structure residing of entire set of samples *via* generating a two-dimensional hierarchy plot called dendrogram. The dendrogram of the 5 examined fruits (Fig. 3A) unveiled two distinctively-separated clusters "1a" corresponding to cumin and anise specimens and cluster "1b" corresponding to fennel, coriander and caraway specimens. Cumin and anise samples were discriminated into two sub-clusters of cluster "1a" confirming their quite compositional divergences.

PCA is a pattern recognition method mainly used to examine data trends using smaller number of dimensions, thus allowing better mapping and visualization of entire set of samples (scores) in addition to exploring the variables with the highest weights related to these samples (loadings). PCA model was prescribed by 3 components explaining 63% of the total variance with clear discrimination of cumin and anise specimens from the other groups. The close grouping of the biological replicates within each specimen denotes for the model validity and moreover the low biological and technical variability (Fig. 3B). Cumin and anise samples exhibited positive values of PC1 and could readily be separated through the PC2 projection (Fig. 3B, right side). However, fennel specimens were partially separated, with negative PC2 score

values, from the segregated non resolved coriander and caraway specimens (Fig. 3B, left side) in accordance with HCA analysis (Fig. 3A). The loading plot (Fig. 3C) revealed metabolites that contributed to fruits segregation pattern. Specifically, fatty acid signals of linolenic, linoleic and oleic acids were more abundant in anise samples. Quercetin-*O*-hexauronide, with negative loading values along PC1 & PC2 was a differential marker enriched in fennel samples. Additionally, the loading plot also revealed MS signals corresponding to metabolites abundant in cumin samples *viz.*, luteolin-*O*-hexosyl hexauronide, apigenin and homo(iso)citric acid, the latter metabolite was detected exclusively in cumin affirming the potential of the developed model.

3.2.2. Supervised OPLS-DA modelling of roasting effect on umbelliferous fruits metabolomes. OPLS-DA is another multivariate data analysis tool that uses a supervised priori knowledge for maximizing class separation rather than explaining the variations within a set of samples. Such model was employed to assess the impact of roasting on three of the examined umbelliferous fruit metabolomes in addition to highlighting the metabolites enriched in roasted fruits *versus* unroasted ones. The developed models exemplified in the score plots (Fig. 4A–C) showed quite effective separation between roasted and unroasted species with excellent fitness and good predictive capacities (cumin; $R^2 = 99.3\%$ and $Q^2 = 74.6\%$, fennel; $R^2 = 99.7\%$ and $Q^2 = 92.4\%$, anise; $R^2 = 99.8\%$ and $Q^2 = 86.7\%$). The inspection of the derived S plot, a tool generated by plotting the covariance against the correlation, revealed key metabolites responsible for distinct variation between the roasted and unroasted specimens (Fig. 4D–F). Quercetin-*O*-hexauronide and apigenin-*O*-hexosyl-malonate were differential markers enriched in unroasted fennel and unroasted cumin specimens, respectively suggesting for the degradation of flavonoid glycosides in agreement with our previous report in *Ceratonia siliqua* pod.[10] Likewise, the S-plot also revealed for a richer fatty acids profile *viz.*, oleic acid (anise), hydroxyoctadecadienoic acid (anise & fennel), linoleic acid (fennel) and hydroxyoctadecenoic acid (cumin) in unroasted samples indicating that roasting catalyzes lipid degradation. Additionally, Maillard type degradation reaction is a plausible explanation for the detection of furan peak (difuranyl-dimethyl-undecatrien-ol) as most distinctive marker in roasted cumin fruit.[11] Several amino acid sugar conjugates *i.e.* (isoleucyl-*O*-hexose) were detected in unroasted anise samples and can serve as precursors for these Maillard products.

3.3. Effect of roasting on TPC, TFC and antioxidant activity of the studied fruits

Although OPLS-DA coupled to UHPLC/MS revealed the roasting impact on some individual metabolites, particularly phenolics and to less extent fatty acids, more generalized approaches are required to assess roasting ultimate impact on fruits' antioxidant activity and in relation to their total phenolics (TPC) and flavonoids content (TFC). Chemical assays *viz.*, TPC, TFC and DPPH˙ radical scavenging assays were utilized for evaluating the roasting effect on cumin, fennel and anise specimens. As depicted in (Fig. 5A), unroasted specimens showed enriched TPC ranging from (0.641 to 0.994 mg GAE per g extract) with the highest levels present in fennel *versus* lowest in anise samples. Upon roasting, TPC dropped sharply with fennel specimens exhibiting the strongest decline (from 0.994 to 0.295 mg GAE

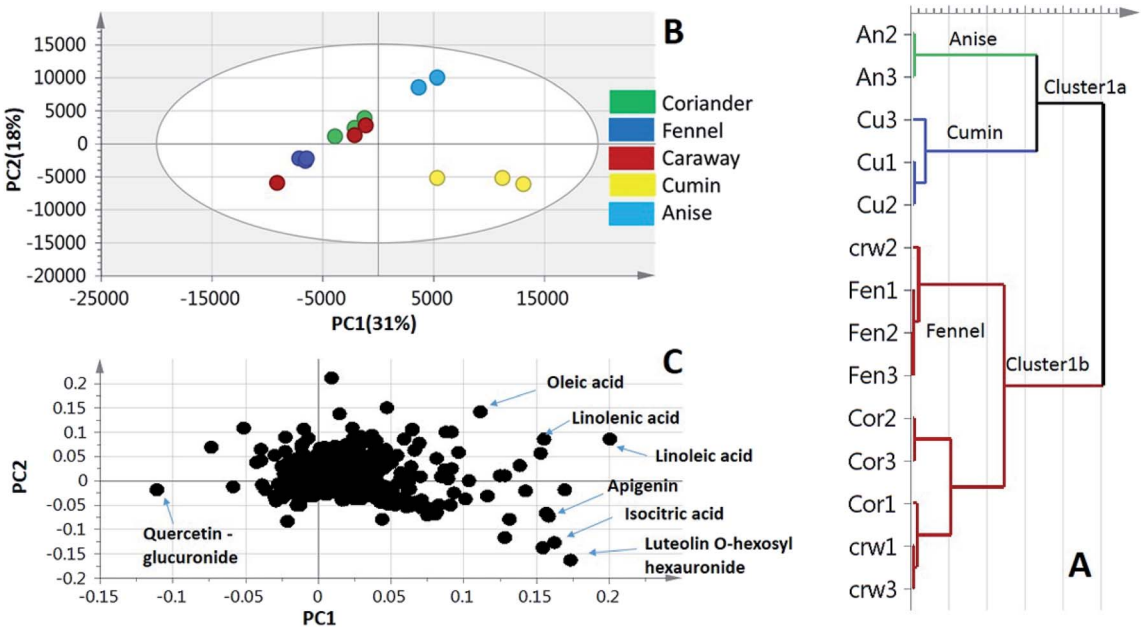

Fig. 3 Unsupervised multivariate data analysis of UHPLC-MS data of the studied umbelliferous fruits. (A) HCA plot (B) PCA score plot of PC1 *vs.* PC2 scores. (C) Loading plot for PC1 & PC2 showing metabolites and their assignments. The unsupervised models showed the partial segregation of the samples and the tight clustering of the biological replicates.

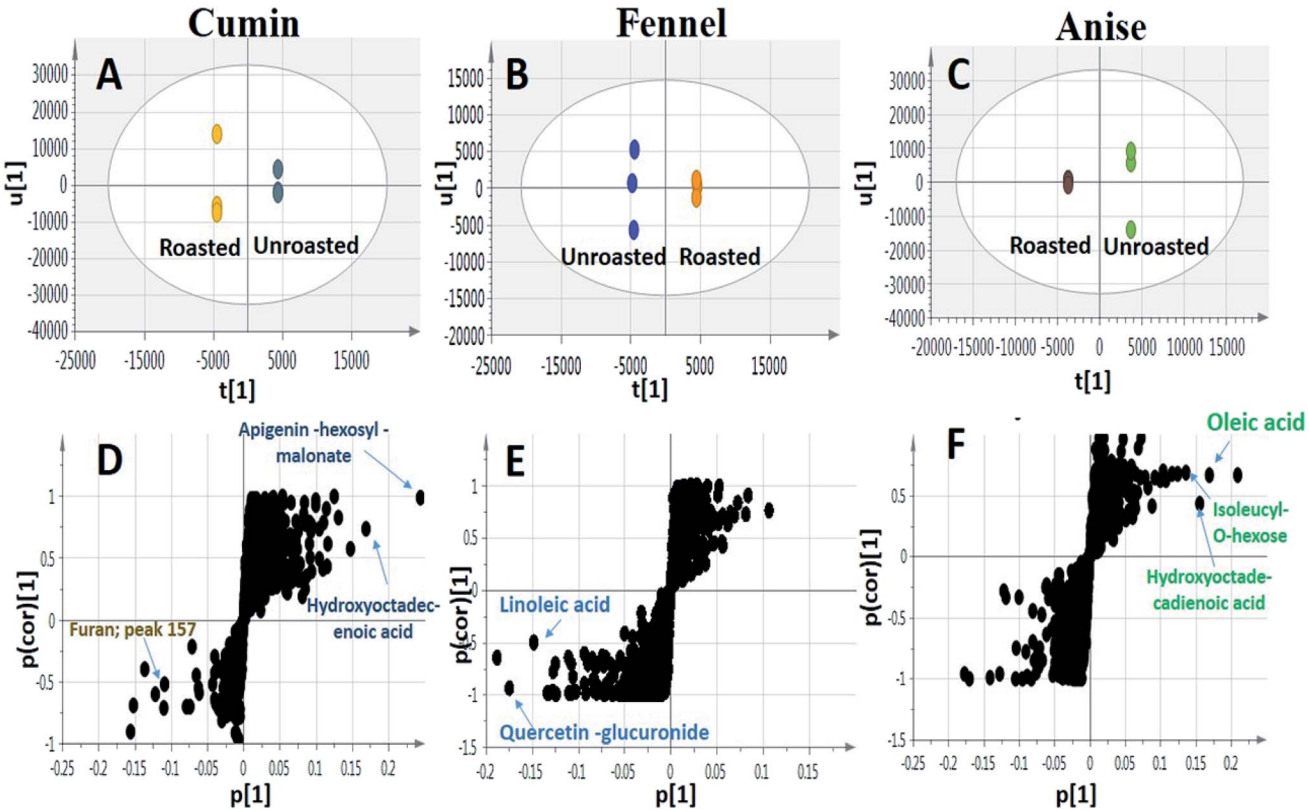

Fig. 4 UHPLC-MS based OPLS-DA score plots derived from modelling roasted against unroasted fruits (A–C). The S-plots (D–F) show the covariance p[1] against the correlation p(cor)[1] of the variables of the discriminating component of the OPLS-DA models. Selected variables are highlighted in the S-plots and their biochemical pathway analysis are discussed in text.

per g extract) which comes in line with a previous report in roasted fennel bulb.[32] Similarly, quantitative determination of TFC (Fig. 5B) revealed that unroasted specimens exhibited comparable TFC ranging (from 0.232 to 0.441 mg QE per g extract) which also decreased upon roasting as exemplified in case of cumin and anise samples. Furthermore, DPPH$^{\bullet}$ free radical scavenging assay revealed that roasted cumin, fennel and anise appeared to be less effective to scavenge DPPH$^{\bullet}$

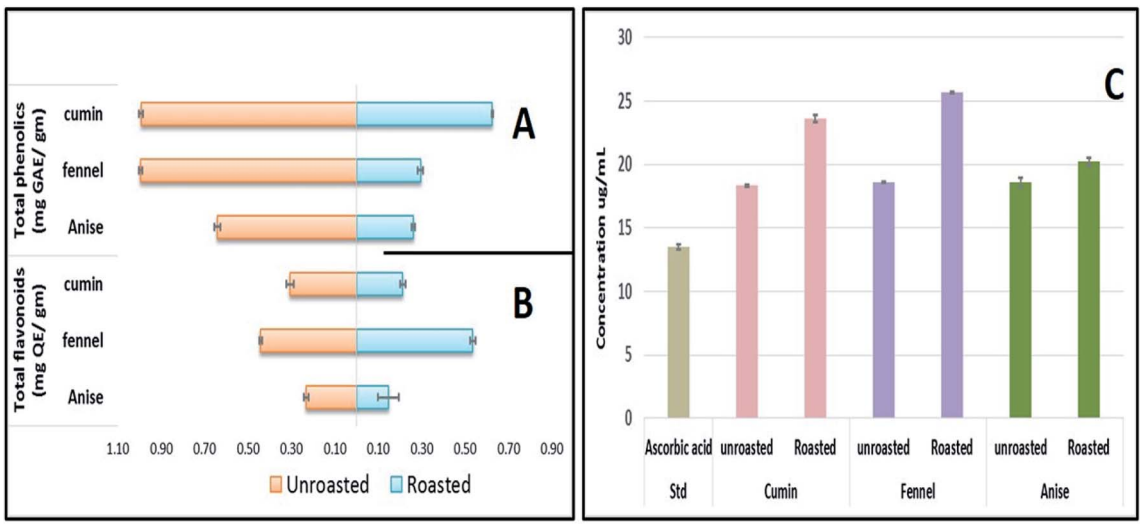

Fig. 5 Total phenolic content (mg gallic acid equivalent/g plant residue) (A), total flavonoid content (mg quercetin equivalent per g plant residue) (B) and DPPH free radical scavenging measured as IC50 (μg mL^{-1}) (C) of cumin, fennel and anise samples before and after roasting. For DPPH$^{\bullet}$ reduction inhibition, higher values correspond to lower activity.

radical exemplified in a higher concentrations required to obtain a 50% radical inhibition compared to its unroasted counterparts (Fig. 5C).

4. Conclusion

In summary, this report represents the first comprehensive secondary metabolite profiling that aims to provide chemical based evidence for the health benefits of umbelliferous spices *viz.*, cumin, fennel, anise, coriander and caraway. Hyphenation of ultra-performance liquid chromatography with high resolution Q-TOF mass analyzer proved to be a superior analytical tool in this study, thus enabled the separation as well as annotation of 186 metabolites mainly predominated by flavonoids, fatty acids and phenolic acids. Furthermore, multivariate data analysis tools were employed to unravel the metabolomics heterogeneity of this taxa genotypes in addition to post roasting. Finally, the relationship between the TPC, TFC and fruits antioxidant activity in roasted and unroasted samples was further investigated where substantially lower antioxidant effects were exhibited in roasted samples. These findings provide further evidence for these spices' value as a source of functional phytoconstituents and explain for the processing impact *i.e.* roasting on its metabolic composition.

Conflicts of interest

There are no conflicts to declare.

Acknowledgements

Dr Mohamed A. Farag acknowledges the funding received from the Alexander von Humboldt Foundation, Germany.

References

1 E. Shawky and R. M. Abou El Kheir, *Phytochem. Anal.*, 2018, **29**, 452–462.
2 B. Sayed-Ahmad, T. Talou, Z. Saad, A. Hijazi and O. Merah, *Ind. Crops Prod.*, 2017, **109**, 661–671.
3 J.-N. Wei, Z.-H. Liu, Y.-P. Zhao, L.-L. Zhao, T.-K. Xue and Q.-K. Lan, *Food Chem.*, 2019, **286**, 260–267.
4 Ö. Ç. Açar, V. Gökmen, N. Pellegrini and V. Fogliano, *Eur. Food Res. Technol.*, 2009, **229**, 961–969.
5 R. Pérez-Míguez, E. Sánchez-López, M. Plaza, M. Castro-Puyana and M. L. Marina, *Anal. Bioanal. Chem.*, 2018, **410**, 7859–7870.
6 F. R. Pinu, *Food Res. Int.*, 2015, **72**, 80–81.
7 M. A. Farag, A. R. Khattab, A. A. Maamoun, M. Kropf and A. G. Heiss, *Food Res. Int.*, 2019, **115**, 379–392.
8 M. Castro-Puyana, R. Pérez-Míguez, L. Montero and M. Herrero, *TrAC, Trends Anal. Chem.*, 2017, **93**, 102–118.
9 I. M. Abu-Reidah, D. Arráez-Román, I. Warad, A. Fernández-Gutiérrez and A. Segura-Carretero, *Food Res. Int.*, 2017, **93**, 87–96.
10 M. A. Farag, D. M. El-Kersh, A. Ehrlich, M. A. Choucry, H. El-Seedi, A. Frolov and L. A. Wessjohann, *Food Chem.*, 2019, **283**, 675–687.
11 C. M. Klevorn and L. L. Dean, *Food Chem.*, 2018, **240**, 1193–1200.
12 M. M. Elmassry, L. Kormod, R. M. Labib and M. A. Farag, *J. Chromatogr. B: Anal. Technol. Biomed. Life Sci.*, 2018, **1099**, 117–126.
13 A. Porzel, M. A. Farag, J. Mülbradt and L. A. Wessjohann, *Metabolomics*, 2014, **10**, 574–588.
14 M. A. Farag and Z. T. A. Shakour, *Phytochemistry*, 2019, **161**, 117–129.
15 I. Blaženović, T. Kind, J. Ji and O. Fiehn, *Metabolites*, 2018, **8**, 31.
16 M. A. Farag and L. A. Wessjohann, *Planta Med.*, 2012, **78**, 488–496.
17 S. Surveswaran, Y.-Z. Cai, H. Corke and M. Sun, *Food Chem.*, 2007, **102**, 938–953.
18 O. U. Shirazi, M. Khattak, N. A. M. Shukri and M. N. Nasyriq, *J. Pharmacogn. Phytochem.*, 2014, **3**, 104–108.
19 J.-J. Macheix, *Fruit Phenolics: 0*, CRC press, 2017.
20 L. Barros, A. M. Carvalho and I. C. Ferreira, *LWT–Food Sci. Technol.*, 2010, **43**, 814–818.
21 T. Watanabe, Y. Arai, Y. Mitsui, T. Kusaura, W. Okawa, Y. Kajihara and I. Saito, *Clin. Exp. Hypertens.*, 2006, **28**, 439–449.
22 M. Farag, S. Ezzat, M. Salama and M. Tadros, *J. Pharm. Biomed. Anal.*, 2016, **125**, 292–302.
23 R. Bernini, F. Crisante and M. C. Ginnasi, *Molecules*, 2011, **16**, 1418–1425.
24 Y. Zhang, H. Ma, W. Liu, T. Yuan and N. P. Seeram, *J. Agric. Food Chem.*, 2015, **63**, 10097–10102.
25 L. J. Leventhal, E. G. Boyce and R. B. Zurier, *Ann. Intern. Med.*, 1993, **119**, 867–873.
26 S. Li, Z. Jiang, L. Thamm and G. Zhou, *J. Am. Soc. Brew. Chem.*, 2010, **68**, 114–118.
27 N. D. Hamilton, *US Pat.*, US6479069B1, 2002.
28 S. Yang, M. Liu, N. Liang, Q. Zhao, Y. Zhang, W. Xue and S. Yang, *Chem. Cent. J.*, 2013, **7**, 24.
29 I. Pugajeva, I. Perkons and P. Górnaś, *J. Food Compos. Anal.*, 2018, **74**, 44–52.
30 P. Kulanthaivel, W. P. Janzen, L. M. Ballas, J. B. Jiang, C.-Q. Hu, J. W. Darges, J. C. Seldin, D. J. Cofield and L. M. Adams, *Planta Med.*, 1995, **61**, 41–44.
31 E. M. Abd El-Kader, A. Serag, M. S. Aref, E. E. A. Ewais and M. A. Farag, *Plant Cell, Tissue Organ Cult.*, 2019, **137**, 309–318.
32 A. Rawson, M. B. Hossain, A. Patras, M. Tuohy and N. Brunton, *Food Res. Int.*, 2013, **50**, 513–518.